

Unification of Landau diamagnetism and de Haas-van Alphen effect for a harmonically trapped Fermi gas in a synthetic magnetic field

Shyamal Biswas,* Avijit Ghosh, and Soumyadeep Majumder

School of Physics, University of Hyderabad, C.R. Rao Road, Gachibowli, Hyderabad-500046, India

(Dated: August 23, 2022)

We have analytically explored artificial magnetism of 3-D spin-polarized harmonically trapped ideal Fermi gas of electrically neutral particles exposed to a constant synthetic magnetic field. We have unified the artificial Landau diamagnetism and the artificial de Haas-van Alphen effect in a single framework for all temperatures as well as for all possible values of the synthetic magnetic field. Our prediction is testable in the present-day experimental setup.

PACS numbers: 75.20.-g (Diamagnetism, paramagnetism, and superparamagnetism), 67.85.-d (Ultracold gases, trapped gases), 05.30.Fk (Fermion systems and electron gas), 05.30.Jp (Boson systems)

I. INTRODUCTION

It is well known that the Coriolis force ($\vec{F}_C = 2\vec{m}\vec{v} \times \vec{\Omega}$) acting on an electrically neutral particle in the rotating frame is analogous to the Lorentz force ($\vec{F}_L = q\vec{v} \times \vec{B}$) acting on a charged particle due to an external magnetic field in a rest frame of reference [1]. This analogy gives rise to the artificial magnetism of a rotating harmonically trapped gas of electrically neutral particles in a rotating frame of reference [2], in particular, when the angular speed of rotation approaches the angular trap frequency ($\Omega \rightarrow \omega_\perp$) [1]. When the angular speed of rotation approaches the angular trap frequency, the trapping effect is cancelled by the centrifugal effect and the problem reduces to the cyclotron motion of a charged particle in a constant magnetic field [1]. This analogy finds application of Landau level physics [3–5], such as the quantum Hall effect [6], in the rotating trapped quantum gases of electrically neutral atoms. However, in reality [2, 7–11], the angular speed of rotation is always less than the angular trap frequency. This is a requirement for the stability of the system in the rotating frame [5]. The significant difference of the centrifugal force ($\vec{m}\Omega^2\vec{r}_\perp$) and the trapping force ($-\vec{m}\omega_\perp^2\vec{r}_\perp$) can drastically change the properties of artificial magnetism because the centrifugal force is analogous to a term $\vec{m}(\frac{qB}{2m})^2\vec{r}_\perp$ nonlinear in artificial magnetic field. Hence it is impossible to study usual Landau diamagnetism [12], de Haas-van Alphen effect [13], *etc* in a rotating trapped Fermi gas of neutral atoms even for $\Omega < \omega_\perp$.

The artificial magnetism can be alternatively studied by exposing harmonically trapped gas of neutral atoms to artificial or synthetic magnetic field. An external artificial magnetic field has already been created for a neutral gas of trapped ultracold atoms [14]. Hereafter any effect related to the artificial magnetic field will be coined as artificial effect over the existing name. Artificial quantum

Hall effect has been observed in such a system of neutral atoms moving perpendicular to the artificial magnetic field [15]. Creation of artificial magnetic field for neutral atoms stimulated a lot of experimental and theoretical progress in the field [16–21]. However, the elementary aspects of the artificial magnetism, such as artificial Landau diamagnetism [12] and artificial de Haas-van Alphen effect [13], have not been observed in trapped gas of neutral fermionic atoms [22, 23] exposed to an artificial magnetic field. A few such elementary aspects, on the other hand, were theoretically explored for both the 2-D Fermi system [24] and the 3-D Fermi system [25, 26] for low temperatures and weak & strong fields. However, unification of the artificial Landau diamagnetism and the artificial de Haas-van Alphen effect have not been even theoretically achieved for all temperatures and fields. Hence we take up the discussion of artificial magnetism of a 3-D harmonically trapped Fermi gas in an artificial magnetic field.

Pauli paramagnetism often comes into the discussion of magnetism in terms of the spin of individual particles (fermions) [27]. The particles we are considering though have individual spin, the spin does not couple with the artificial magnetic field. Hence we are not discussing the artificial Pauli paramagnetism. On the other hand, Pauli paramagnetism, Landau diamagnetism and de Haas-van Alphen effect have been unified for all temperatures and all values of the magnetic field for an ideal homogeneous gas of electrons exposed to a uniform magnetic field [28]. We adopt and extend the method described in Ref.[28] for the unification of the artificial Landau diamagnetism and the artificial de Haas-van Alphen effect for all temperatures and all possible values of the artificial magnetic field.

Calculation in this article begins with the energy eigenvalues of the single-particle Hamiltonian of a 3-D harmonically trapped charge neutral ideal Fermi gas exposed to a uniform artificial magnetic field. We consider cylindrical symmetry of harmonic oscillations. We also consider that the artificial magnetic field be applied to the axis of the cylindrical symmetry. We calculate the grand

*Electronic address: [sbsp\[at\]uohyd.ac.in](mailto:sbsp[at]uohyd.ac.in)

free energy of the Fermi gas. We unify the artificial Landau diamagnetism and the artificial de Haas-van Alphen effect in a single framework for all temperatures and all values of the artificial magnetic field. Here-from we evaluate magnetic moment of the Fermi gas. We plot artificial magnetic field dependence of the magnetic moment of the Fermi system. We show cross-over of the de Haas-van Alphen oscillation and the saturation in this regard. Finally, we conclude.

II. GRAND FREE ENERGY FOR A ROTATING HARMONICALLY TRAPPED IDEAL QUANTUM GAS

Let us consider a 3-D harmonically trapped ideal Fermi gas of particles in thermodynamic equilibrium with a heat and particle reservoir of temperature T and chemical potential μ . Let the average total number of particles in the gas be N . Let the mass and charge of each particle of the gas be \bar{m} and q , respectively. We consider the (angular) trap frequency to be the same (ω_{\perp}) for oscillations along the x -axis and that along the y -axis. Let us now apply a uniform artificial magnetic field $\vec{B} = B\hat{k}$ to the Fermi system along the z -axis. Single-particle Hamiltonian of the system under the application of the artificial magnetic field becomes [14]

$$H = \frac{(\vec{p} - q\vec{A})^2}{2\bar{m}} + \frac{1}{2}\bar{m}\omega_{\perp}^2 r_{\perp}^2 + \frac{1}{2}\bar{m}\omega_z^2 z^2 \quad (1)$$

where \vec{p} is the generalized momentum of a particle, q is the artificial charge of the particle which either can be set to 1 or can be absorbed to \vec{A} [5], $\vec{A} = -\frac{1}{2}\vec{r} \times B\hat{k}$ is the artificial gauge field, $\vec{r} = x\hat{i} + y\hat{j} + z\hat{k}$ is the position the particle, \vec{r}_{\perp} is the position of the particle in the $x-y$ plane, ω_z is the trap frequency of the particle along the z -axis.

Energy eigenvalues for the single-particle Hamiltonian of the system with respect to the lab-fixed (non-rotating) frame are given by the combination of the Fock-Darwin energy levels[34] and 1-D simple harmonic oscillator energy levels[35], as [29]

$$\epsilon_{n,m,j} = (n + 1/2)\hbar(\sqrt{\omega_{\perp}^2 + \Omega_B^2} + \Omega_B) + (m + 1/2) \times \hbar(\sqrt{\omega_{\perp}^2 + \Omega_B^2} - \Omega_B) + (j + 1/2)\hbar\omega_z \quad (2)$$

where $\Omega_B = \frac{qB}{2\bar{m}}$ is half of the cyclotron frequency, $n = 0, 1, 2, \dots$ represents the Landau level quantum number for $\omega_{\perp} \rightarrow \Omega_B$, $n - m = n, n - 1, n - 2, \dots$ represents the magnetic quantum number for $m = 0, 1, 2, \dots$, and $j = 0, 1, 2, \dots$ represents 1-D simple harmonic oscillator energy level quantum number. Grand free energy of the Fermi system is given by

$$\Phi = -k_B T \sum_{n=0}^{\infty} \sum_{m=0}^{\infty} \sum_{j=0}^{\infty} \ln(1 + e^{-[\epsilon_{n,m,j} - \mu]/k_B T}). \quad (3)$$

Taylor expansion of the above logarithm about $e^{\mu/k_B T} = 0$ and successive evaluation of the above summations, results in [30]

$$\Phi = -k_B T \left[\sum_{l=1}^{\infty} \frac{(-1)^{l-1} z^l}{l} \frac{1}{2 \sinh\left(\frac{l\hbar[\sqrt{\omega_{\perp}^2 + \Omega_B^2} + \Omega_B]}{2k_B T}\right)} \times \frac{1}{2 \sinh\left(\frac{l\hbar[\sqrt{\omega_{\perp}^2 + \Omega_B^2} - \Omega_B]}{2k_B T}\right)} \frac{1}{2 \sinh\left(\frac{l\hbar\omega_z}{2k_B T}\right)} \right] \quad (4)$$

where $z = e^{\mu/k_B T}$ is the fugacity of the system. This result is exact for all temperatures and angular speeds of rotation.

The average total number of particles ($N = -\frac{\partial \Phi}{\partial \mu}|_{T, \omega_{\perp}, \omega_z, \Omega_B}$) in the system can be obtained from Eqn.(4), as [30]

$$N = \sum_{l=1}^{\infty} (-1)^{l-1} z^l \frac{1}{2 \sinh\left(\frac{l\hbar[\sqrt{\omega_{\perp}^2 + \Omega_B^2} + \Omega_B]}{2k_B T}\right)} \times \frac{1}{2 \sinh\left(\frac{l\hbar[\sqrt{\omega_{\perp}^2 + \Omega_B^2} - \Omega_B]}{2k_B T}\right)} \frac{1}{2 \sinh\left(\frac{l\hbar\omega_z}{2k_B T}\right)}. \quad (5)$$

This form of the average total number of particle, however, can be simplified in the thermodynamic limit and in the limiting case of $\Omega_B \rightarrow 0$, as

$$N \simeq \left(\frac{k_B T}{\hbar\bar{\omega}}\right)^3 (-)\text{Li}_3(-z) \quad (6)$$

where $\bar{\omega} = [\omega_{\perp}^2 \omega_z]^{1/3}$ is the geometric mean of the trap frequencies and $\text{Li}_{\nu}(z) = z + \frac{z^2}{2^{\nu}} + \frac{z^3}{3^{\nu}} + \dots$ is the polylogarithmic function of the order ν and argument z . Here, by the thermodynamic limit, we mean $N \rightarrow \infty$, $\frac{\hbar\omega_{\perp}}{k_B T} \rightarrow 0$, $\frac{\hbar\omega_z}{k_B T} \rightarrow 0$ and $\frac{\hbar\bar{\omega}}{k_B T} N^{1/3} = \text{constant}$. The fugacity, as well as the chemical potential, is usually determined from Eqn.(6) in terms of T , ω and N in the thermodynamic limit for $\Omega_B \rightarrow 0$ [31]. However, extraction of the properties of the artificial magnetism needs to go beyond $\Omega_B \rightarrow 0$ limit. The fugacity, as well as the chemical potential, depends on the angular speed of rotation for fixed T , ω and N , according to Eqn.(5) for any nonzero value of Ω_B .

III. ARTIFICIAL MAGNETIC MOMENT OF THE UNCHARGED FERMIONS IN THE ROTATING HARMONIC TRAP

The artificial magnetic moment of the system of our interest can be defined by $\vec{M} = -\frac{\partial \Phi}{\partial \vec{B}}|_{\mu, T} = -\hat{k} \frac{q}{2\bar{m}} \frac{\partial \Phi}{\partial \Omega_B}|_{\mu, T}$. From Eqn.(4), by following this definition, we get magnitude of the artificial magnetic moment of the ideal gas of uncharged fermions in the rotating harmonic trap with

respect to the lab-fixed frame, as

$$M = \frac{\hbar q}{2\bar{m}} \left[\sum_{l=1}^{\infty} \frac{(-1)^{l-1} z^l \operatorname{csch}(\frac{l\hbar\omega_z}{2k_B T})}{4} \times \frac{\sqrt{\omega_{\perp}^2 + \Omega_B^2} \sinh(\frac{l\hbar\Omega_B}{k_B T}) - \Omega_B \sinh(\frac{l\hbar\sqrt{\omega_{\perp}^2 + \Omega_B^2}}{k_B T})}{\sqrt{\omega_{\perp}^2 + \Omega_B^2} [\cosh(\frac{l\hbar\Omega_B}{k_B T}) - \cosh(\frac{l\hbar\sqrt{\omega_{\perp}^2 + \Omega_B^2}}{k_B T})]^2} \right]. \quad (7)$$

This form of artificial magnetic moment is exact in all respects. This form, of course, takes the finite-size effect into account. It is expected that the artificial magnetic moment would be proportional to the total number of particles, at least, in the thermodynamic limit. Exact form of the artificial magnetic moment per particle (fermion) can now be obtained from Eqns.(7) and (5), as

$$\frac{M}{N} = \frac{\hbar q}{2\bar{m}} \left[\sum_{l=1}^{\infty} \frac{(-1)^{l-1} z^l \operatorname{csch}(\frac{l\hbar\omega_z}{2k_B T})}{4} \times \frac{\sqrt{\omega_{\perp}^2 + \Omega_B^2} \sinh(\frac{l\hbar\Omega_B}{k_B T}) - \Omega_B \sinh(\frac{l\hbar\sqrt{\omega_{\perp}^2 + \Omega_B^2}}{k_B T})}{\sqrt{\omega_{\perp}^2 + \Omega_B^2} [\cosh(\frac{l\hbar\Omega_B}{k_B T}) - \cosh(\frac{l\hbar\sqrt{\omega_{\perp}^2 + \Omega_B^2}}{k_B T})]^2} \right] / \left[\sum_{l=1}^{\infty} (-1)^{l-1} z^l \frac{1}{2 \sinh(\frac{l\hbar[\sqrt{\omega_{\perp}^2 + \Omega_B^2} + \Omega_B]}{2k_B T})} \right] \times \frac{1}{2 \sinh(\frac{l\hbar[\sqrt{\omega_{\perp}^2 + \Omega_B^2} - \Omega_B]}{2k_B T})} \frac{1}{2 \sinh(\frac{l\hbar\omega_z}{2k_B T})}. \quad (8)$$

This equation suggests that the artificial magnetic moment of the system has a saturation value $-M_s$ where $M_s = N \frac{\hbar q}{2\bar{m}}$. The saturation value is, of course, reached at $B \rightarrow \infty$. Plotting of Eqn.(8) with respect to the angular speed to rotation needs the chemical potential to be evaluated from Eqn.(5) as a function of N , T , Ω_B , and the trap frequencies. However, we fix the chemical potential as it is for $\Omega_B \rightarrow 0$ for the plotting of Eqn.(8) with respect to the artificial magnetic field. We plot Eqn.(8) (solid line) in figure 1 for the parameters as shown in the plot-label and the figure caption. These parameters, in particular, ω_z , ω_{\perp} and T_F are taken from the experimental values for $N = 3 \times 10^5$ [5]. It is clear from figure 1 that the artificial magnetic moment is negative and reaches saturation at a higher value of the angular speed of rotation. This result is analogous to the phenomenon of orbital magnetism. For the case of the low temperature and the rapid rotation of the system, the artificial magnetic moment would be found to be oscillating due to the existence of alternating series of the powers z ($\gg 1$) in Eqn.(7). This phenomenon would be coined as the artificial de Haas-van Alphen effect.

A. Artificial Landau diamagnetism

We recast Eqn.(8) to the lowest leading order in Ω_B after the Laurent series expanding the hyperbolic func-

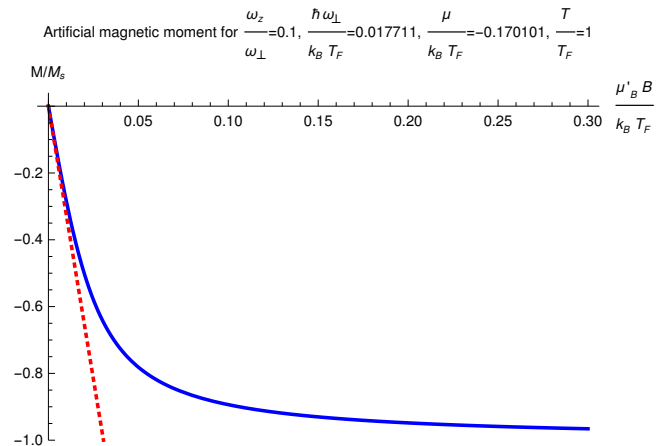


FIG. 1: Plot of the artificial magnetic moment versus angular speed of rotation for the rotating trapped ideal Fermi gas for the Fermi temperature $T_F = 27.0976 \mu\text{K}$ [5]. While the solid line follows Eqn.(8), the dotted line follows Eqn.(9).

tions (e.g. $\sinh(x) = x + \frac{x^3}{3!} + \frac{x^5}{5!} + \dots$ and $\cosh(x) = \frac{1}{x} - \frac{x}{6} + \frac{7x^3}{360} - \dots$), as

$$M \simeq -M_s \frac{-\operatorname{Li}_2(-z)}{-\operatorname{Li}_3(-z)} \frac{\hbar\Omega_B}{3k_B T} = -M_s \frac{-\operatorname{Li}_2(-z)}{-\operatorname{Li}_3(-z)} \frac{\mu'_B B}{3k_B T} \quad (9)$$

where $\mu'_B = \frac{\hbar q}{2\bar{m}}$ has the dimension of the Bohr magneton. This result corresponds to Landau diamagnetism. Temperature dependence of the fugacity of Eqn.(9) can be determined from Eqn.(6). There-from it can be shown that $\frac{-\operatorname{Li}_2(-z)}{-\operatorname{Li}_3(-z)} \rightarrow 1$ for $T \rightarrow \infty$. Hence Eqn.(9) follows Curie's law at the high temperatures. For $T \rightarrow 0$, on the hand, we have $\frac{-\operatorname{Li}_2(-z)}{-\operatorname{Li}_3(-z)} \rightarrow \frac{3T}{T_F}$ [36] according to the Sommerfeld's asymptotic expansions of both the numerator (Fermi-Dirac integral of order 2) and the denominator (Fermi-Dirac integral of order 3) [31]. Thus for $T \rightarrow 0$, the artificial magnetic moment varies as $M \simeq -M_s \frac{\mu'_B B}{k_B T_F}$ to the lowest leading order in B . We plot Eqn.(9) (dotted line) in figure 1 for the parameters same as that for the solid line in the same figure. Linearity of the plot with B and negative values of M confirms the existence of the artificial Landau diamagnetism in the rotating trapped ideal Fermi gas of uncharged particles. This result would, however, be okay for $\frac{\mu'_B B}{k_B T_F} \ll 1$. The solid line in the same figure, on the other hand, captures the finite-size effect and the higher order effect of B , and consequently, exhibits the saturation of the artificial magnetic moment of the system.

B. Artificial de Haas-van Alphen effect

Artificial magnetic field dependence of the artificial magnetic moment would be completely different at low

temperatures and high angular speeds. Artificial de Haas-van Alphen oscillation would be observed in this regime. We will, however, investigate the same in the thermodynamic limit. Properties of the artificial de Haas-van Alphen effect is supposed to be extracted from Eqn.(7) because it represents an exact result even for low temperatures and high angular speeds. Although Eqn.(7) is plausible for high temperatures and low angular speeds of rotation, it is not plausible for low temperatures due to the existence of a pole type singularity in M/N at either $T \rightarrow 0$ or at $\Omega_B \rightarrow \infty$. We can avoid such a problem by recasting the grand free energy in Eqn.(4) for low temperatures and strong artificial magnetic fields.

Since we have $\frac{1}{2 \sinh(x/2)} = \frac{e^{-x/2}}{1-e^{-x}} \forall x \in \mathbb{R}$, we recast Eqn.(4), as

$$\Phi = -k_B T \left[\sum_{l=1}^{\infty} \frac{(-1)^{l-1} z^l}{l} \frac{e^{-\frac{l\hbar[\sqrt{\omega_{\perp}^2 + \Omega_B^2} + \Omega_B]}{2k_B T}}}{1 - e^{-\frac{l\hbar[\sqrt{\omega_{\perp}^2 + \Omega_B^2} + \Omega_B]}{k_B T}}} \right. \\ \left. \times \frac{e^{-\frac{l\hbar[\sqrt{\omega_{\perp}^2 + \Omega_B^2} - \Omega_B]}{2k_B T}}}{1 - e^{-\frac{l\hbar[\sqrt{\omega_{\perp}^2 + \Omega_B^2} - \Omega_B]}{k_B T}}} \frac{e^{-\frac{l\hbar\omega_z}{2k_B T}}}{1 - e^{-\frac{l\hbar\omega_z}{k_B T}}} \right]. \quad (10)$$

The above equation can be further recast by truncating Taylor expansions of the exponentials in the last two fractions and performing binomial expansion of $\frac{1}{1 - e^{-\frac{l\hbar[\sqrt{\omega_{\perp}^2 + \Omega_B^2} + \Omega_B]}{k_B T}}}$ as

$$\Phi \simeq -k_B T \left[\sum_{l=1}^{\infty} \frac{(-1)^{l-1} z^l}{l} \frac{1}{\frac{l\hbar[\sqrt{\omega_{\perp}^2 + \Omega_B^2} - \Omega_B]}{k_B T}} \frac{1}{\frac{l\hbar\omega_z}{k_B T}} \right. \\ \left. \times e^{-\frac{l\hbar[\sqrt{\omega_{\perp}^2 + \Omega_B^2} + \Omega_B]}{2k_B T}} \sum_{k=1}^{\infty} e^{-\frac{l(k-1)\hbar[\sqrt{\omega_{\perp}^2 + \Omega_B^2} + \Omega_B]}{2k_B T}} \right] \\ \simeq -\frac{(k_B T)^3 [\sqrt{\omega_{\perp}^2 + \Omega_B^2} + \Omega_B]}{\hbar^2 \omega_{\perp}^2 \omega_z} \\ \times \sum_{k=1}^{\infty} (-) \text{Li}_3 \left(-e^{-\frac{\mu - (k-1)\hbar\Omega_B - k\hbar\sqrt{\omega_{\perp}^2 + \Omega_B^2}}{k_B T}} \right). \quad (11)$$

in the thermodynamic limit. Here-from we get the average total number of particles ($N = -\frac{\partial \Phi}{\partial \mu}|_{T, \omega_{\perp}, \omega_z, \Omega_B}$) as

$$N \simeq \frac{(k_B T)^2 [\sqrt{\omega_{\perp}^2 + \Omega_B^2} + \Omega_B]}{\hbar^2 \omega_{\perp}^2 \omega_z} \\ \times \sum_{k=1}^{\infty} (-) \text{Li}_2 \left(-e^{-\frac{\mu - k\hbar\sqrt{\omega_{\perp}^2 + \Omega_B^2} - (k-1)\hbar\Omega_B}{k_B T}} \right). \quad (12)$$

Exact expression of magnitude of the artificial magnetic moment ($\vec{M} = -\frac{\partial \Phi}{\partial \vec{B}}|_{\mu, T} = -\hat{k} \frac{q}{2m} \frac{\partial \Phi}{\partial \Omega_B}|_{\mu, T}$) can be ob-

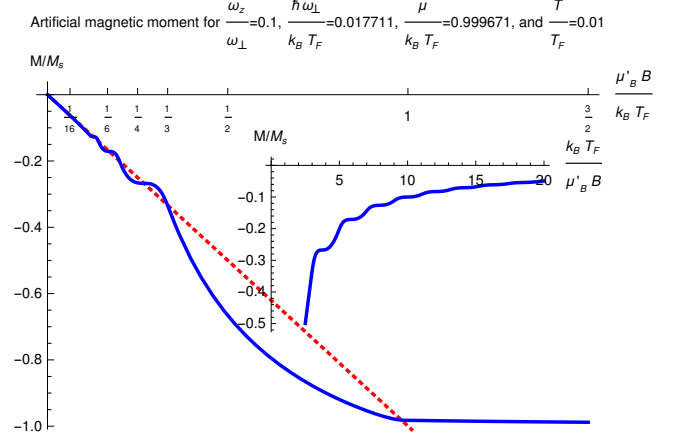


FIG. 2: Plot of the Artificial magnetic moment versus angular speed of rotation for the rotating trapped ideal Fermi gas for the Fermi temperature $T_F = 27.0976 \mu\text{K}$ [5]. The solid line follows Eqn.(14). The dotted line follows Eqn.(9). The solid line in the inset also follows Eqn.(14).

tained from Eqn.(10), as

$$M = \frac{-\hbar q}{2m} \sum_{l=1}^{\infty} \frac{(-1)^{l-1} e^{\frac{\mu - l\hbar\sqrt{\omega_{\perp}^2 + \Omega_B^2}}{k_B T}}}{\left[1 - e^{-\frac{l\hbar[\sqrt{\omega_{\perp}^2 + \Omega_B^2} - \Omega_B]}{k_B T}}\right]^2 \left[1 - e^{-\frac{l\hbar[\sqrt{\omega_{\perp}^2 + \Omega_B^2} + \Omega_B]}{k_B T}}\right]^2} \\ \times \frac{e^{-\frac{l\hbar\omega_z}{2k_B T}}}{1 - e^{-\frac{l\hbar\omega_z}{k_B T}}} \left(\frac{\Omega_B}{\sqrt{\omega_{\perp}^2 + \Omega_B^2}} \left[1 - e^{-\frac{2l\hbar\sqrt{\omega_{\perp}^2 + \Omega_B^2}}{k_B T}}\right] \right. \\ \left. - \left[e^{-\frac{l\hbar[\sqrt{\omega_{\perp}^2 + \Omega_B^2} - \Omega_B]}{k_B T}} - e^{-\frac{l\hbar[\sqrt{\omega_{\perp}^2 + \Omega_B^2} + \Omega_B]}{k_B T}} \right] \right). \quad (13)$$

It is clear from the above equation that the artificial magnetic moment of the system is always negative. It is also clear from the terms in the parenthesis of the above equation that the artificial magnetic moment would be linear in Ω_B for small Ω_B s as expected from the artificial Landau diamagnetism.

Now approximating $\frac{e^{-\frac{l\hbar\omega_z}{2k_B T}}}{1 - e^{-\frac{l\hbar\omega_z}{k_B T}}}$ as $\frac{1}{\frac{l\hbar\omega_z}{k_B T}}$, $\frac{1}{\left[1 - e^{-\frac{l\hbar[\sqrt{\omega_{\perp}^2 + \Omega_B^2} - \Omega_B]}{k_B T}}\right]^2}$ as $\frac{1}{\left[\frac{l\hbar[\sqrt{\omega_{\perp}^2 + \Omega_B^2} - \Omega_B]}{k_B T}\right]^2}$, bi-nomial expanding $\frac{1}{\left[1 - e^{-\frac{l\hbar[\sqrt{\omega_{\perp}^2 + \Omega_B^2} + \Omega_B]}{k_B T}}\right]^2}$ as $\sum_{k=1}^{\infty} k e^{-\frac{(k-1)l\hbar[\sqrt{\omega_{\perp}^2 + \Omega_B^2} + \Omega_B]}{k_B T}}$, and evaluating the summation over l , we recast Eqn.(13) with the further

use of Eqn.(12), as

$$\begin{aligned} \frac{M}{N} \simeq & -\frac{\hbar q}{2\bar{m}} \frac{k_B T}{\hbar[\sqrt{\omega_\perp^2 + \Omega_B^2} - \Omega_B]} \left[\sum_{k=1}^{\infty} \left(\frac{\Omega_B}{\sqrt{\omega_\perp^2 + \Omega_B^2}} \times \right. \right. \\ & \left. \left[(-)\text{Li}_3 \left(-e^{\frac{\mu - \hbar[k\sqrt{\omega_\perp^2 + \Omega_B^2} + (k-1)\Omega_B]}{k_B T}} \right) \right. \right. \\ & \left. \left. - (-)\text{Li}_3 \left(-e^{\frac{\mu - \hbar[(k+2)\sqrt{\omega_\perp^2 + \Omega_B^2} + (k-1)\Omega_B]}{k_B T}} \right) \right] \right. \\ & \left. + \left[(-)\text{Li}_3 \left(-e^{\frac{\mu - \hbar[(k+1)\sqrt{\omega_\perp^2 + \Omega_B^2} + k\Omega_B]}{k_B T}} \right) \right. \right. \\ & \left. \left. - (-)\text{Li}_3 \left(-e^{\frac{\mu - \hbar[(k+1)\sqrt{\omega_\perp^2 + \Omega_B^2} + (k-2)\Omega_B]}{k_B T}} \right) \right] \right) \right] / \\ & \left[\sum_{k=1}^{\infty} (-)\text{Li}_2 \left(-e^{\frac{\mu - k\hbar\sqrt{\omega_\perp^2 + \Omega_B^2} - (k-1)\hbar\Omega_B}{k_B T}} \right) \right] \quad (14) \end{aligned}$$

in the thermodynamic limit. Eqn.(14) represents the artificial magnetic moment per particle of the Fermi system. This equation is useful for describing the artificial de Haas-van Alphen effect for strong artificial magnetic fields. This equation is also useful for describing the artificial magnetism for weak artificial magnetic fields in the thermodynamic limit. Eqn.(12) becomes same as Eqn.(6) once the summation over k is replaced by integration over k in the thermodynamic limit for $\Omega_B \rightarrow 0$. Now we evaluate the chemical potential from Eqn.(6) according to the method described in Ref.[31]. We plot the artificial magnetic moment of Eqn.(14) in figure 2 (solid line) with respect to the artificial magnetic field for the parameters same as that used in figure 1 except the temperature $T = 0.01 T_F$ and chemical potential $\mu = 0.999671 k_B T_F$. We also plot the artificial magnetic moment of Eqn.(9) (dotted) line in the same figure for the same parameters as mentioned in the plot-label and the figure caption. We also plot the artificial magnetic moment with respect to inverse of the artificial magnetic field in the inset of figure 2 for same set of parameters. Oscillations in the artificial magnetic moment about its weak field results, which are indicated by the dotted line, represent the artificial de Haas-van Alphen effect. While the de Haas-van Alphen oscillations are observed periodically with the inverse of the external magnetic field in a gas (metal) of free electrons [31], the artificial de Haas-van Alphen oscillations are not periodic rather quasi-periodic due to the inhomogeneity of the Fermi system as clear from the inset of figure 2. Both the artificial Landau diamagnetism and the artificial de Haas-van Alphen effect are described by the solid line in figure 2. Hence Eqn.(14) unifies the artificial Landau diamagnetism and the artificial de Haas-van Alphen effect in the thermodynamic limit.

However, if we compare figure 1 and figure 2, then we can safely say that the artificial de Haas-van Alphen

effect dominates at a low temperature ($T \ll T_F$) and high speed of rotation ($\hbar\Omega_B \lesssim k_B T_F$).

IV. CONCLUSION

To conclude, we have unified Landau diamagnetism and de Haas-van Alphen effect for the artificial magnetism of a harmonically trapped Fermi gas in a synthetic magnetic field. Our unification is applicable for all temperatures, as well as for all strengths of the synthetic magnetic field. Our predictions are observable within the existing experimental set-up [5].

We could study artificial magnetism rotating harmonically trapped Bose gas of uncharged particles. All the results would be unaltered for this case except the replacement of $(-1)^l z^l$ by z^l and the replacement of $-\text{Li}(-x)$ by $\text{Li}(x) \forall x \in \mathbb{R}$. However, necessary condition for observing the artificial de Haas-van Alphen effect would be $\mu > \epsilon_{0,0,0}$. Such a condition is not reached by a Bose system. Hence one can not observe artificial de Haas-van Alphen effect in a Bose system.

Properties of rotating trapped Bose and Fermi systems are often analysed from the body-fixed rotating frame of reference. We have, however, analysed the properties from the lab-fixed (non-rotating) frame. Centrifugal force additionally appears in the rotating frame and consequently, changes the entire physics because of appearance of a pole type singularity at $\Omega_B \rightarrow \omega_\perp$ in the grand free energy. It also brings the question of stability of the system in the rotating frame for $\Omega_B \geq \omega_\perp$. We would not get the artificial Landau diamagnetism, as well as Curie's law, in the rotating frame. Artificial de Haas-van Alphen effect would also be very much different in the rotating frame.

Pauli paramagnetism, Landau diamagnetism, and de Haas-van Alphen effect have already been unified for an ideal and homogeneous gas of electrons. Our consideration of only one component of spin of the uncharged fermionic atoms stopped us studying the Pauli paramagnetism. One component of the spin is required for trapping the atoms in a magneto-optical trap [32, 33]. However, how to unify Pauli paramagnetism, Landau diamagnetism, and de Haas-van Alphen effect for the artificial magnetism, is kept as an open problem.

Acknowledgement

S. Biswas acknowledges partial financial support of the SERB, DST, Govt. of India under the EMEQ Scheme [No. EEQ/2019/000017]. Useful discussions with Prof. J. K. Bhattacharjee (IACS, Kolkata) and Mr. Samir Das (UoH, Hyderabad) are gratefully acknowledged.

-
- [1] G. Juzeliūnas, *Physics* **2**, 25 (2009)
- [2] Y.-J. Lin, R. L. Compton, A. R. Perry, W. D. Phillips, J. V. Porto, and I. B. Spielman, *Phys. Rev. Lett.* **102**, 130401 (2009)
- [3] L. D. Landau and E. M. Lifshitz, *Quantum Mechanics*, 3rd ed., Sec. 112, p. 458, Butterworth-Heinemann, Oxford (1980)
- [4] V. Schweikhard, I. Coddington, P. Engels, V. P. Mogen-dorff, and E. A. Cornell *Phys. Rev. Lett.* **92**, 040404 (2004)
- [5] S. Stock, B. Battelier, V. Bretin, Z. Hadzibabic, and J. Dalibard, *Laser Phys. Lett.* **2**, 275 (2005)
- [6] N. K. Wilkin and J. M. F. Gunn, *Phys. Rev. Lett.* **84**, 6 (2000)
- [7] M. R. Matthews, B. P. Anderson, P. C. Haljan, D. S. Hall, M. J. Holland, J. E. Williams, C. E. Wieman, and E. A. Cornell, *Phys. Rev. Lett.* **83**, 3358 (1999)
- [8] K. W. Madison, F. Chevy, W. Wohlleben, and J. Dalibard, *Phys. Rev. Lett.* **84**, 806 (2000)
- [9] J. R. Abo-Shaer, C. Raman, J. M. Vogels, and W. Ketterle, *Science* **292**, 476 (2001)
- [10] P. C. Haljan, I. Coddington, P. Engels, and E. A. Cornell, *Phys. Rev. Lett.* **87**, 210403 (2001)
- [11] M. W. Zwiernik, J. R. Abo-Shaer, A. Schirotzek, C. H. Schunck, and W. Ketterle, *Nature* **435**, 1047 (2005)
- [12] L. D. Landau, *Z. Phys.* **64**, 629 (1930); L. D. Landau and E. M. Lifshitz, *Statistical Physics*, Part 1, 3rd ed., sec. 59 and 60, p. 171-176, Butterworth-Heinemann, Oxford (1980)
- [13] W. J. de Haas and P. M. van Alphen, *Proc. Netherlands Roy. Acad. Sci.* **33**, 680 (1930)
- [14] Y.-J. Lin, R. L. Compton, K. Jiménez-García, J. V. Porto, and I. B. Spielman, *Nature* **462**, 628 (2009)
- [15] L. J. LeBlanc, K. Jiménez-García, R. A. Williams, M. C. Beeler, A. R. Perry, W. B. Phillips, and I. B. Spielman, *PNAS* **109**, 10811 (2012)
- [16] I. B. Spielman, *Phys. Rev. Lett.* **79**, 063613 (2009)
- [17] J. Dalibard, F. Gerbier, G. Juzeliūnas, and P. Öhberg, *Rev. Mod. Phys.* **83**, 885 (2011)
- [18] D. Jaksch, *Physics* **5**, 60 (2012)
- [19] M.-X. Huo, W. Nie, D. A. W. Hutchinson, L. C. Kwek, *Scientific Reports* **4**, 5992 (2014)
- [20] Z.-F. Yu, F.-Q. Hu, A.-X. Zhang, J.-K. Xue, *Phys. Lett. A* **380**, 789 (2016)
- [21] D. Babik, R. Roell, D. Helten, M. Fleischhauer, and M. Weitz, *Phys. Rev. A* **101**, 053603 (2020)
- [22] S. Chaturvedi and S. Biswas, *Resonance* **19**, 45 (2014)
- [23] S. Biswas, D. Jana, and R. K. Manna, *Eur. Phys. J. D* **66**, 217 (2012)
- [24] B. Farias and C. Furtado, *Physica B* **481**, 19 (2016)
- [25] T. Suzuki, H. Imamura, M. Hayashi, and H. Ebisawa, *J. Phys. Soc. Jpn.* **71**, 1242 (2002)
- [26] Y. Li, *Physica B* **481**, 38 (2016)
- [27] W. Pauli, *Z. Phys.* **41**, 81 (1927)
- [28] S. Biswas, S. Sen, and D. Jana, *Phys. Plasmas* **20**, 052503 (2013)
- [29] V. Halonen, *Solid State Commun.* **92**, 703 (1994)
- [30] S. Dey, P. Manchala, S. Basu, D. Banerjee, and S. Biswas, *Phys. Scr.* **95**, 075003 (2020)
- [31] S. Biswas and D. Jana, *Eur. J. Phys.* **33**, 1527 (2012)
- [32] L. P. Pitaevskii, S. Stringari, *Bose-Einstein Condensation*, Clarendon Press, Oxford (2003)
- [33] S. Giorgini, L. P. Pitaevskii, and S. Stringari, *Rev. Mod. Phys.* **80**, 1215 (2008)
- [34] Fock-Darwin energy levels are linked to $\sqrt{\omega_{\perp}^2 + \Omega_B^2} \pm \Omega_B$ for the rotational and harmonic motion in the $x-y$ plane.
- [35] Simple harmonic oscillator's energy levels are linked to ω_z for the harmonic motion along the z -axis.
- [36] $T_F = \frac{\hbar\omega_{[6N]}^{1/3}}{k_B}$ is the Fermi temperature of the system.